IEEE Access
Multidisciplinary | Rapid Review | Open Access Journal

Received September 15, 2017, accepted November 15, 2017, date of publication November 22, 2017,
date of current version December 22, 2017.

*Digital Object Identifier 10.1109/ACCESS.2017.2776349*

# Adaptive Image Contrast Enhancement by Computing Distances into a 4-Dimensional Fuzzy Unit Hypercube

**MARIO VERSACI[1], (Senior Member, IEEE),**
**FRANCESCO CARLO MORABITO[1], (Senior Member, IEEE),**
**AND GIOVANNI ANGIULLI[2], Senior Member, IEEE)**
[1]Department of Civil, Energy, Environmental and Materials Engineering, Mediterranea University of Reggio Calabria,89122 Reggio Calabria, Italy
[2]Department of Information, Infrastructures and Sustainable Energy Engineering, Mediterranea University of Reggio Calabria, 89122 Reggio Calabria, Italy

Corresponding author: Giovanni Angiulli (giovanni.angiulli@unirc.it)

**ABSTRACT** A new fuzzy procedure for adaptive gray-level image contrast enhancement (CE) is presented in this paper. Starting from the pixels belonging to a normalized gray-level image, an appropriate smooth S-shaped fuzzy membership function (MF) is considered for gray-scale transformation and is adaptively developed through noise reduction and information loss minimization. Then, a set of fuzzy patches is extracted from the MF, and for each support of each patch, we compute four ascending-order statistics that become points inside a 4-D fuzzy unit hypercube after a suitable fuzzification step. CE is performed by computing the distances among the above points and the points of maximum darkness and maximum brightness (special vertexes in the hypercube), and by determining the rotation of the tangent line to the MF around a crucial point where fuzzy patches and the MF coexist. The proposed procedure enables high CE in all the treated images with performance that is fully comparable with that obtained by three more sophisticated fuzzy techniques and by standard histogram equalization.

**INDEX TERMS** Image processing, adaptive contrast enhancement, fuzzy logic, fuzzy unit hypercubes, over-/under-enhancement.

## I. INTRODUCTION

Within *image processing* (*IP*), *contrast enhancement* (*CE*) improves image data by stretching the distribution of the gray levels using adaptive techniques that directly and automatically process the extracted features [1]–[3]. Many *CE* techniques have been developed based on the type of information to be highlighted. Mathematical morphology, for example, is a mature technique for extracting shape and size information from an image that involves configuration of a set of nonlinear operators (dilation and erosion) that act on images using structuring elements [4], [5]. By contrast, the top hat transformation is considered to be a good technique to extract bright or dark features smaller than a given size from an uneven background [6]. Both single-scale and multi-scale morphological filtering have been successfully exploited in local contrast enhancement, producing good visual results in terms of contrast [4], [6]. In [7]–[9], for example, good results were obtained by power-law transformation and saturation operators, which resulted in good quality in the modified images. Furthermore, substantial effort has been made to remove noise while preserving the edges [10], [11]. *CE* techniques based on histogram equalization (*HE*) are the most popular because of their simplicity and the meaningful results [12]–[15]. This technique, which is based on flattening and stretching the dynamic range of the image's histogram, can achieve overall *CE* but may sometimes reduce the local details and result in over-enhancement. Accordingly, specific *HE* techniques, such as contrast-limited adaptive histogram equalization, which splits the image into tiles on which *HE* is applied and combines the neighboring tiles by bilinear interpolation to eliminate artificially induced boundaries and emphasize local contrast rather than overall contrast, have been developed [16]. In addition, taking into account the input histogram separation approach, several techniques have been developed based on the mean gray level (brightness-preserving bi-*HE*), the median gray level (dualistic sub-image *HE*), and the maximum gray level (minimum mean brightness error


2169-3536 © 2017 IEEE. Translations and content mining are permitted for academic research only.
Personal use is also permitted, but republication/redistribution requires IEEE permission.
See http://www.ieee.org/publications_standards/publications/rights/index.html for more information.

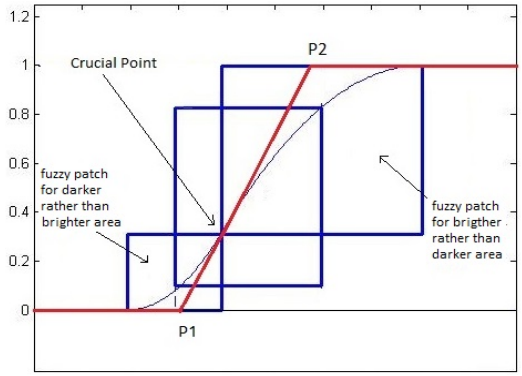


**FIGURE 1.** ***S*-function covered by $FP_1$, $FP_2$, $FP_3$ (gray, dark and bright zones) and the new *S – function* produced by the proposed procedure (red line). Two cusps, $P_1$ and $P_2$, are clearly shown.**

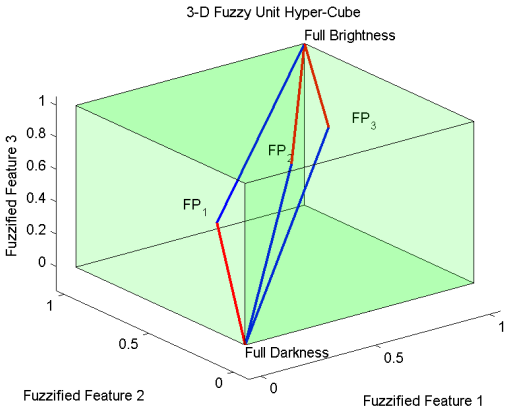


**FIGURE 2.** ***FFs* inside a *n – UKC*.**

Bi-*HE*) [1], [17]. However, the techniques mentioned above do not consider the fact that the sampling techniques and the transition zones of a gray level image often feature from uncertainty and vagueness, so it may be useful to treat images with fuzzy approaches. In particular, the logarithmic function [18], fuzzy entropy approaches [19]–[21] and fuzzy similarity indexes [22] have been successfully exploited for gray level fuzzification and to capture the neighborhood characteristics. In addition, appreciable results have been achieved through fuzzy-wavelet procedures using approximation and detail coefficients together with transformation and saturation operators to transfer images remotely [23]–[26]. In such a context, owing to the development of a geometrical fuzzy procedure that makes the approach "readable" and helpful for non-technical experts, in this paper, inspired by [27], we propose a new fuzzy approach based on the combined exploitation of a 4-dimensional fuzzy unit hypercube (*FUHC*), noise reduction and information loss minimization to enhance gray level images. A smooth S-shaped fuzzy membership function (*MF*), which is adaptively set by techniques based on both noise reduction and information loss minimization, fuzzifies the gray level image. Then, the input-output space of the *MF* is covered by a set of partially overlapped *fuzzy patches* (*FPs*) (Fig. 1) seeking within that space a *crucial point* (*CP*) (i.e., the point of maximal ambiguity with membership values falling around 0.5) on which to modify the *MF*. From the *supports* of each *FP*, we extract 4 statistical *features* (*F*) that, after appropriate fuzzification, become 4-dimensional points inside a *FUHC* (or 4-unit Kosko's cube ($4 - UKC$)) [28]. Two particular points lie inside each $4 - UKC$: the total brightness and total darkness (Fig. 2). If the *fuzzified features* (*FFs*) are closer to the total brightness point, they are considered brighter rather than darker, and the *MF* slope around the *CP* is increased by a factor depending on that distance. Conversely, if the *FFs* are closer to the total darkness point, then they are considered darker rather than brighter, and the *MF* slope around the *CP* is reduced by a factor depending on that distance (for details, see Fig. 3).

When applied to a set of low-contrast images, satisfying results, largely comparable with those obtained by using established techniques, are achieved. The rest of this paper is organized as follows. After a quick overview of fuzzy set theory for *IP* (Section II), the materials and methods are detailed, leading to the exploitation of $n - FUHC$ to set and edit the parameters characterizing the *CE* (Section III). The approach is applied to a set of low-contrast gray level images with different features, and each operational choice is justified by comparing the results with those obtained by other established fuzzy techniques, such as those presented in [18], [19], and [21], and with the standard histogram equalization procedure (Section IV). Finally, in Section V, some conclusions and future perspectives are discussed.

## II. FUZZY SET THEORY FOR IMAGE PROCESSING (*FIP*)

Proposed as an extension of classic set theory, fuzzy set theory addresses problems with inherent vagueness and/or imprecision in the shading of the membership of each element to a given set in the range [0, 1] by a membership function (*MF*) that manages its fuzziness. Formally, a fuzzy set $A$ is defined by the ordered pair $(U, h(U))$, where $U$ is the universe of discourse (all possible values defining $A$), and $h(u) : U \rightarrow [0, 1]$, $u \in U$, defining the membership value of $u$ to $A$. Fuzzy *IP* (*FIP*) usually follows three steps: fuzzification, inference engine and defuzzification. Fuzzification maps an image from the *pixel plane* (*PP*) to the *fuzzy plane* (*FPL*) over which the image enhancement is performed (inference engine). Finally, defuzzification maps the modified image from the *FP* to the *PP*. If $x_{ij}$ is a gray-level pixel of an original image (*OI*) whose brightness is $L(x_{ij}) \in [0, 255]$, setting $L_{min} = 0$ and $L_{max} = 255$, then the image can be formalized as

$$\begin{cases} \sum_{i=1}^{M-1} \sum_{j=1}^{N-1} [x_{ij}, L_{norm}(x_{ij})] \\ \forall x_{ij} \in OI, \quad i = 0, \ldots, M-1, \; j = 0, \ldots, N-1, \end{cases}$$

where $L_{norm}(x_{ij}) = y_{ij} = \frac{L(x_{ij})}{L_{max}} \in [0, 1]$, $i = 0, 1, \ldots, M-1$, *and* $j = 0, 1, \ldots, N-1$ are the normalized gray

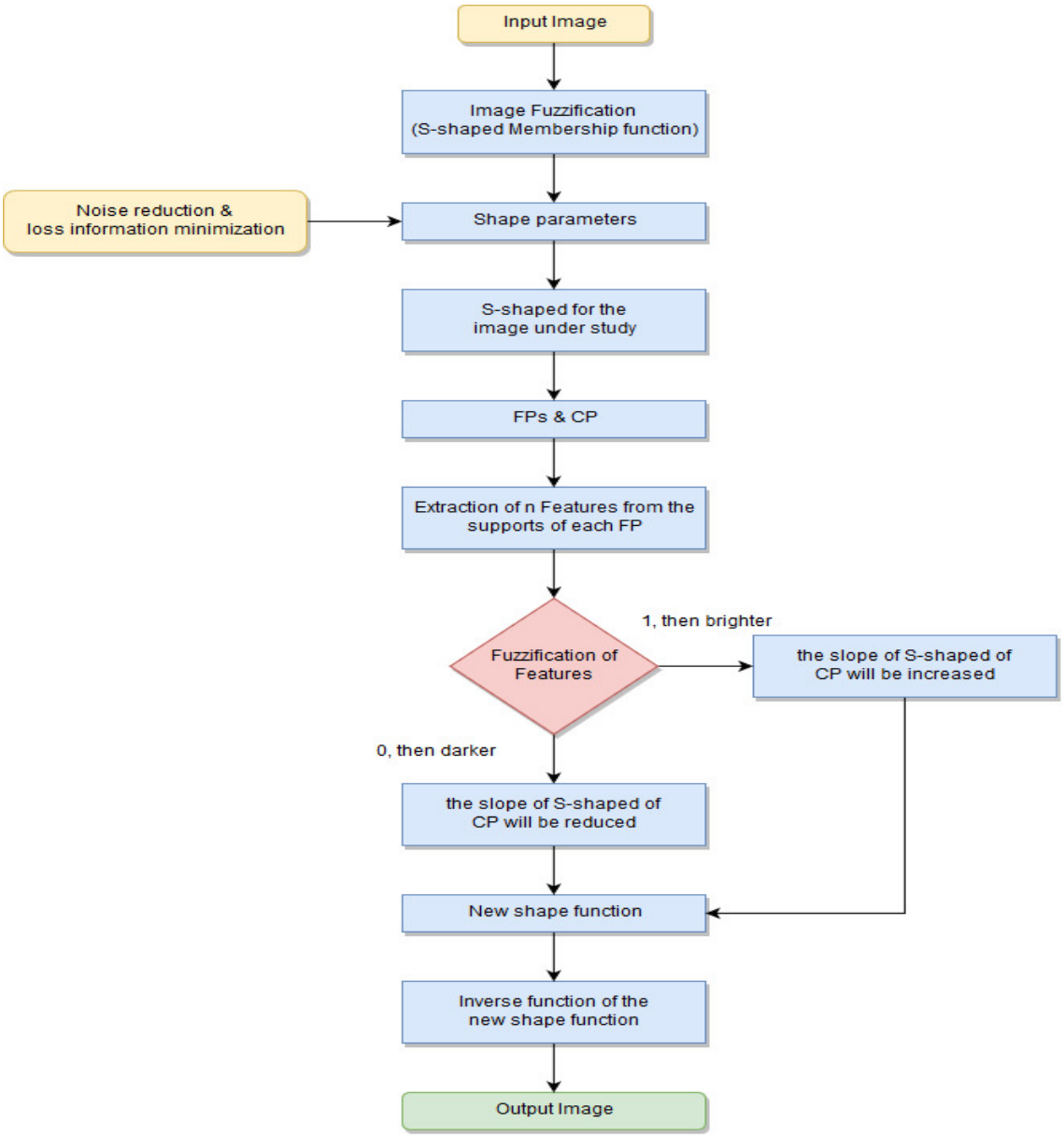


**FIGURE 3.** Flow chart of the proposed procedure.

levels. In addition, a fuzzy $MF$, $h_{ij} = h(y_{ij}) : I \rightarrow [0, 1]$, formalizes the membership of $y_{ij}$ to $OI$ such that:

$$\begin{cases} h_{ij} = 0 & \text{if } y_{ij} \notin OI \text{ (totally)}, \\ h_{ij} = 1 & \text{if } y_{ij} \in OI \text{ (totally)}. \end{cases}$$

Intermediate values of $h_{ij}$ indicate partial membership of the related pixel. Therefore, $CE$ can be defined as an $h_{ij}$ transformation to obtain the modified image on the $FPL$.

## III. MATERIALS AND METHODS

To explain the details of the proposed procedure, in this section, we introduce some definitions exploited in the following.

*Definition 1 (Fuzzy Contrast Enhancement (FCE)):* By considering *dark*, *light* and *gray* as instances of fuzzy quantities, we define a smooth shape function, $S(\cdot)$, that, starting from a normalized $OI$, fuzzifies the information content and modifies its values:

$$S = S(h_{ij}) \quad h_{ij} \in OI \text{ normalized},$$

to obatin an image on a $FPL$ over which $CE$ is performed. Thus, the shape parameters, $S(h_{ij})$, have to be adaptively computed to achieve the best performance. In particular, if $\underline{c}$ is a $k$-dimensional vector defining such parameters, then $S$ is dependent on both $h_{ij}$ and $\underline{c}$. In this paper, $\underline{c}$ is computed via noise reduction and information loss minimization.

*Definition 2 (Fuzzy Paches (FPs) and Supports):* By *FPs*, we denote geometrical spots, e.g., rectangular spots that are partially superimposed and completely cover $S$ (Fig. 1). If $|\{FPs\}| = m$, then

$$\{FPs\} = \{(FP)_j, j = 1, \ldots, m \ni' (FP)_j \subseteq U \times [0, 1]\}.$$

The following characterization ensures partial overlap among consecutive *FPs*: 1) $\{FPs\}$ are a covering of the $S$-function (labeled by $A$); and 2) consecutive *FPs* are partially superimposed. Formally:

$$\bigcup_j (FP)_j \supseteq A; \ (FP)_k \cap (FP)_l \neq \emptyset, \quad k = l + 1.$$

We orthogonally project each $FP_j$ over both $U$ and $[0, 1]$ and determine closed and limited $Support_j$ and $u_j$ characterized by (Fig. 1):

$$\begin{cases} (FP)_j = Support_j \times u_j \\ Support_j \subset U \\ u_j \subseteq [0, 1]; \quad Support_k \cap Support_l \neq \emptyset; \ u_k \cap u_l \neq \emptyset, \end{cases}$$

with $k = l + 1$.

*Definition 3 (Crucial Point (CP)):* For the *FPL*, the membership value equal to 0.5 is the most critical because it is the site of maximum uncertainty. Therefore, this point plays a major role in the proposed procedure. Formally, we define *CP* as the $h_{ij}$ value corresponding to the fuzzy value equal to 0.5, i.e., $CP = h_{ij} \ni' S(h_{ij}) = 0.5$. $S(h_{ij})$ is modified around this point, as detailed below. Each $Support_j$ must be fuzzified and, after the extraction of an $n$-dimensional vector of features, transformed into a point falling in a particular $n$-dimensional space ($n - UKC$).

*Definition 4 (Features (Fs) of Supports):* $\forall$ $Support_j$ we extract $n$ statistical $F$ to characterize each by a set of real parameters. Therefore, $Features_j \in \mathbb{R}^n \quad \forall j = 1, \ldots, m$ have to be fuzzified, for example, by a *sigmoidal function*, $Sig([\cdot])$,[1] whose argument $[\cdot]$ is $n-$ dimensional to obtain the *fuzzified features* (*FFs*) that, inside the $n - UKC$, represent $n-$dimensional points so that *FCE* is treated by computation of distances inside the $n - UKC$ (Fig. 2). The *FFs* can be formalized as

$$Sig([Features_j]) = [FF_j] \in n - UKC, \quad \forall j = 1, \ldots, m.$$

*Definition 5 (Kosko's Hypecube n − UKC):* Kosko's hypercube ($n - UKC$) is a unitary orthogonal $n$-dimensional cube [28]: $n - UKC = [0, 1]_1 \times [0, 1]_2 \times ... \times [0, 1] \subseteq \mathbb{R}^n$. Each $[FF_j]$ inside $n - UKC$ is a point, $FF_j$, such that:

1) the nearer $FF_j$ is to point zero ($0_{n-UKC}$, maximal darkness point), the darker $FP_j$ is considered to be;
2) the nearer $FF_j$ is to the unitary point ($1_{n-UKC}$, maximal brightness point), the brighter $FP_j$ is.

Therefore, both $0_{n-UKC}$ and $1_{n-UKC}$ strongly influence the shape function so that $distance(FF_j, 1_{n-UKC})$ indicates how far $FF_j$ is from total brightness and $distance(FF_j, 0_{n-UKC})$ measures how far $FF_j$ is from total darkness.

Since *CP* is the maximal fuzziness point, *FCE* is obtained after considering, on *CP*, the tangent line to the *S-shaped membership function* ($S - SMF$) ($t-$line for short), whose slope increases (or decreasing) according to the following criterion: if $FF_j$ is close to $1_{n-UKC} \Rightarrow FP_j$, it is brighter:

$$Slope_{new} = Slope_{old} \times \frac{distance(FF_j, 1_{n-UKC})}{distance(FF_j, 0_{n-UKC})}; \quad (1)$$

conversely, if $FF_j$ is close to $0_{n-UKC} \Rightarrow FP_j$, it is darker:

$$Slope_{new} = Slope_{old} \times \frac{distance(FF_j, 0_{n-UKC})}{distance(FF_j, 1_{n-UKC})}, \quad (2)$$

where $Slope_{old}$ and $Slope_{new}$ are the $t-$line slopes before and after (1) and (2), respectively. (1) and (2) can be taken into account *iff* both denominators are $\neq 0$, and it is imperative to guarantee that $Slope_{new}$ is still limited. The following theorem, whose proof is reported in the appendix, meets these requirements.

*Theorem 1 ( ):* If Eqs. (1) and (2) are satisfied, surely:

$$\begin{cases} distance(FF_j, 0_{n-UKC}) \neq 0 \\ distance(FF_j, 1_{n-UKC}) \neq 0 \\ 0 < Slope_{new} < \infty. \end{cases} \quad (3)$$

### A. MAPPING OF THE OI INTO FPL

For our application, to achieve good smoothing transition quality among gray levels, let us consider an $S$-shaped membership function ($S - SMF$) defined as follows (Fig. 1):

$$\begin{cases} h_{ij} = 0, \ \text{ if } \ 0 \leq y_{ij} \leq c_1; \\ h_{ij} = \dfrac{(y_{ij} - c_1)^2}{(c_2 - c_3) \cdot (c_3 - c_1)} \ \text{ if } \ c_1 \leq y_{ij} \leq c_2; \\ h_{ij} = 1 - \dfrac{(y_{ij} - c_3)^2}{(c_3 - c_2) \cdot (c_3 - c_1)} \ \text{ if } \ c_2 \leq y_{ij} \leq c_3; \\ h_{ij} = 1 \ \text{ if} y_{ij} \geq c_3, \end{cases} \quad (4)$$

where $c_1$, $c_2$ and $c_3$ are the $S - SMF$ shape parameters that are determined adaptively as described below.

### B. ADAPTIVE PROCEDURE FOR SETTING THE S − SMF PARAMETERS

Since $c_1$ and $c_3$ are external values, they are adaptively computed by noise reduction while $c_2$ is evaluated by entropy maximization (located around a gray level whose membership value falls in the neighborhood of 0.5). Starting from [19], let us consider the gray level distribution over the *FPL* whose histogram $H_{ist}(h)$ has $s$ peaks, $\{H_{ist}(h_1), H_{ist}(h_2), \ldots, H_{ist}(h_s)\}$, with weighted mean

$$(Y_{ist_{max}}(h))_{mean} = \frac{\sum_{i=1}^{z} H_{ist_{max}}(h_i) \cdot h_i}{\sum_i^z h_i},$$

[1] Other types of fuzzifying function can be considered depending on the application under study.

where $Y_{ist_{max}}(h)$ is the height of the center of gravity of the histogram.[2] Starting from the $s$ peaks, we consider $t$ peaks ($t \leq s$) larger than $(Y_{ist_{max}}(h))_{mean}$, ruling out the others because they are less meaningful. From this new set of peaks, we select the minimum and maximum values, $(Y_{ist_{min}}(h_1))_{mean}$ and $(Y_{ist_{max}}(h_t))_{mean}$, so that the gray levels with $h$ such that $h < (Y_{ist_{min}}(h_1))_{mean}$ are considered as the background while gray levels with $h > (Y_{ist_{max}}(h_1))_{mean}$ are considered as noise preserving. Taking into account that the loss of information of an $OI$ occurs in the neighborhood of the endpoints of the gray level range, we identify two characteristic gray levels to determine $GL_1$ and $GL_2$, such that $GL_1 < GL_2$, and consider the ranges $[h_{min}, GL_1]$ and $[GL_2, h_{max}]$ on which the information loss is equal to a fixed "ad hoc" value $0 < f_1 < 1$. $GL_1$ and $GL_2$ are produced by verification of the following equalities:

$$\sum_{i=h_{min}}^{GL_1} H_{ist}(i) = f_1; \quad \sum_{i=GL_2}^{h_{max}} H_{ist}(i) = f_1.$$

Finally, $c_1$ and $c_3$ are obtained by

$$c_1 = \frac{h_{max} - h_{min}}{2} + h_{min} and \quad c_3 = \frac{h_{max} - h_k}{2} + h_k$$

with two further conditions:

$$if\ (c_1 > GL_1) \rightarrow c_1 = B_1; \quad if\ (c_1 > GL_1) \rightarrow c_1 = B_1.$$

After computing $c_1$ and $c_3$, if $c_2 \in (c_1, c_3)$, the entropy of an $FI$ will depend on both $FI$ and $\underline{c}$ as:

$$Entropy = Entropy(FI, c_1, c_2, c_3) \tag{5}$$

with

$$S(h_{min}) \leq c_1 < c_2 < c_3 \leq S(h_{max}),$$

where $c_{2_{optimal}}$ is computed by maximization of Eq. (5).

### C. EDITING OF THE S-FUNCTION

We now split $[c_1, c_3]$ into three superimposed sub-ranges to create $FP_1$, $FP_2$ and $FP_3$ (Fig.1): $FP_1$ and $FP_3$ represent darker and brighter zones of the $OI$, respectively. To underline the fuzzy nature of the procedure, $FP_1$ and $FP_3$ have a common vertex located at $U$ with fuzzy membership equal to 0.5 (maximal fuzziness) so that $FP_2$ is centered on a fuzzy membership equal to 0.5 characterizing the gray zones. In this way,

$$\begin{cases} Support_{FP_1} = \dfrac{c_2 + c_3}{2} - \dfrac{c_1 + c_2}{2}; \\ Support_{FP_2} = c_2 - c_1; \\ Support_{FP_3} = c_3 - c_2. \end{cases}$$

[2]In [19], this computation was obtained by

$$(Y_{ist_{max}}(h))_{mean} = \frac{1}{s}\sum_{i=1}^{s} H_{ist_{max}}(h_i),$$

but no weighted mean of $H_{ist_{max}}(h_i)$ was taken into account, which could be determinant for a correct $FCE$.

$\forall\ Support_j, j = FP_1, FP_2, FP_3$, we address our attention to the fourth-order statistics exploiting $F_j$ as a $4-D$ vector

$$\underline{F_j} = [stat_i(Support_j)], \quad i = 1, 2, 3, 4,$$

where $stat_1(\cdot)$ is the arithmetic average; $stat_2(\cdot)$ is the variance; $stat_3(\cdot)$ is the skewness; and $stat_4(\cdot)$ is the kurtosis index. Therefore, $\underline{F_j}$ (with $j = FP_1, FP_2, FP_3$) represents three points over $\mathbb{R}^4$ that, after fuzzification by a sigmoid function, for $j = FP_1, FP_2, FP_3$, gives us three $4-D$ vectors

$$\underline{FF_j} = \left[\frac{1}{1 + e^{-u(F_j - w)}}\right] \in 4 - UKC \quad i = 1, 2, 3, 4,$$

so the new $S - SMF$ is edited by evaluating the distances between $\underline{FF_j}$ and both $0_n - UKC$ and $1_n - UKC$. After evaluating $\underline{FF_j}$ ($j = FP_1, FP_2, FP_3$), the mutual distances in $n - UKC$ can easily be computed as

$$\begin{cases} distance(\underline{FF_m}, \underline{FF_n}) = ||\underline{FF_m}, \underline{FF_n}||_2 \\ m, n = FP_1, FP_2, FP_3. \end{cases}$$

Clearly, two of the following cases could be true. 1) If $FP_1$ represents a brighter zone rather than a darker zone, then the following inequality holds:

$$||\underline{FF}_1 - \underline{FF}_2||_2 > ||\underline{FF}_1 - \underline{FF}_3||_2. \tag{6}$$

2) If $FP_1$ is related to a darker zone rather than a brighter zone, the inequality assumes the following form:

$$||\underline{FF}_1 - \underline{FF}_2||_2 < ||\underline{FF}_1 - \underline{FF}_3||_2. \tag{7}$$

The editing of the $S$-function is performed through anticlockwise rotation of the tangent line ($t - line$ for short) to the $S - SMF$ in $CP$ (point of overlap between darkness and brightness, where $FP_1$, $FP_2$, $FP_3$ and $S - SMF$ coexist). If $FP_1$ is bright rather than dark, $\underline{FF}_1$ is both next to $1_{n-UKC}$ and further away from $0_{n-UKC}$, increasing the slope of $t - line$ by a factor equal to:

$$\frac{||\underline{FF}_1 - 1_{n-UKC}||_2}{||\underline{FF}_1 - 0_{n-UKC}||_2}. \tag{8}$$

Similarly, if $FP_1$ is considered darker rather than brighter, then the $t - line$ slope is decreased by a factor equal to:

$$\frac{||\underline{FF}_1 - 0_{n-UKC}||_2}{||\underline{FF}_1 - 1_{n-UKC}||_2}. \tag{9}$$

In any case, a new $t - line$, labeled $rot - line$, is adaptively generated. Over the Cartesian plane, the $CP$ coordinates can be written as $(c_2, (c_2 - c_1)/(c_3 - c_1))$, so the $t - line$ equation can be written as

$$t - line(h_{ij}) = \frac{c_2 - c_1}{c_3 - c_1} + \frac{2}{c_3 - c_1}\left(h_{ij} - c_2\right).$$

Taking into account both (6) and (8), the $rot$-line slope assumes the form

$$rot - line_{Slope} = t - line_{Slope} + t - line_{Slope}$$

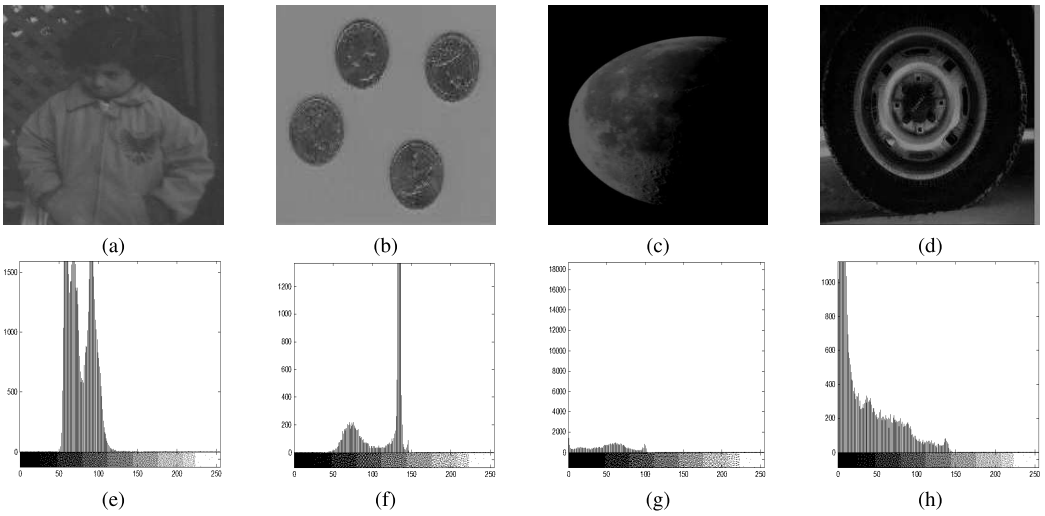


**FIGURE 4.** (a) Portrait representative of Class I (Image 1 in text); (b) A set of coins representing Class II (Image 2 in text); (c) Small bright areas in large dark are are highlighted in this image chosen to represent Class III (Image 3 in text); (d) Image with high alternation of bright and dark areas chosen to represent Class IV (Image 4 in text). (e) to (h) show the histograms for (a) to (d), respectively.

$$\cdot \frac{||\underline{FF}_1 - 1_{n-UKC}||_2}{||\underline{FF}_1 - 0_{n-UKC}||_2} = \frac{2}{c_3 - c_1}\left(1 + \frac{||\underline{FF}_1 - 1_{n-UKC}||_2}{||\underline{FF}_1 - 0_{n-UKC}||_2}\right),$$

so its equation immediately follows:

$$rot - line(h_{ij}) = \frac{c_2 - c_1}{c_3 - c_1} + \frac{2}{c_3 - c_1} \cdot \left(1 + \frac{||\underline{FF}_1 - 1_{n-UKC}||_2}{||\underline{FF}_1 - 0_{n-UKC}||_2}\right)(h_{ij} - b).$$

Finally, to fully define $S - SMF$, we must identify points $P_1$ and $P_2$, and the intersection of the *rot*-line with both the line of membership values equal to zero and the line of membership values equal to unity (Fig.1):

$$P_1 = \left( \underbrace{c_2 + \frac{c_1 - c_2}{2 \cdot (1 + \frac{||\underline{FF}_1 - 1_{n-UKC}||_2}{||\underline{FF}_1 - 0_{n-UKC}||_2})}}_{h_{P_1}}, 0 \right) \text{ and}$$

$$P_2 = \left( \underbrace{\left(1 - \frac{c_2 - c_1}{c_3 - c_1}\right) \cdot \frac{c_1 - c_2}{\frac{2}{c_3 - c_1}\left(1 + \frac{||\underline{FF}_1 - 1_{n-UKC}||_2}{||\underline{FF}_1 - 0_{n-UKC}||_2}\right)}}_{h_{P_2}}, 1 \right),$$

where the gray levels are indicated by $h_{P_1}$ and $h_{P_2}$, $h_{P_1} < h_{P_2}$.[3] Finally, the new $S - SMF$ function, shown in Fig. 1, can be written as follows:

$$\begin{cases} 0 & h_{ij} \le h_{P_1} \\ \frac{c_2 - c_1}{c_3 - c_1} + \frac{2}{c_3 - c_1} \cdot \\ \cdot \left(1 + \frac{||\underline{FF}_1 - 1_{n-UKC}||_2}{||\underline{FF}_1 - 0_{n-UKC}||_2}\right) \cdot (h_{ij} - p_2) & h_{P_1} \le h_{ij} \le h_{P_2} \\ 1 & h_{ij} \ge h_{P_2}. \end{cases} \quad (10)$$

Finally, we obtain the enhanced $OI$ by defuzzification. Specifically, by applying the inverse function of (10), we obtain the fuzzy gray levels (ranging over $[0, 1]$); then, we convert the fuzzy gray levels into the equivalent levels ranging over $[0, 255]$. When patch $FP_1$ is considered darker rather than brighter, it is sufficient to follow the same process (including fuzzification procedure), by carefully considering the inequality (7) with decreased factor (9), to obtain similar equations.

## IV. EXPERIMENTAL RESULTS

Four distinct classes of images of the same size with different contrast characteristics are considered. The database includes 35 low-contrast images belonging to four classes:

1) Class I contains low-contrast portraits;
2) Class II contains images with few areas with medium gray levels;
3) Class III contains images with large dark areas and small bright areas;
4) Class IV contains images with alternating small bright and dark areas.

The procedure is implemented on an Intel Core 2 1.47 GHz CPU in MatLab R2013. The results for the different images are comparable, so we present the results of a single image for each Class (labeled Image 1, Image 2, Image 3 and

[3] $h_{P_1}$ will never be equal to $h_{P_2}$ by virtue of the previous theorem.

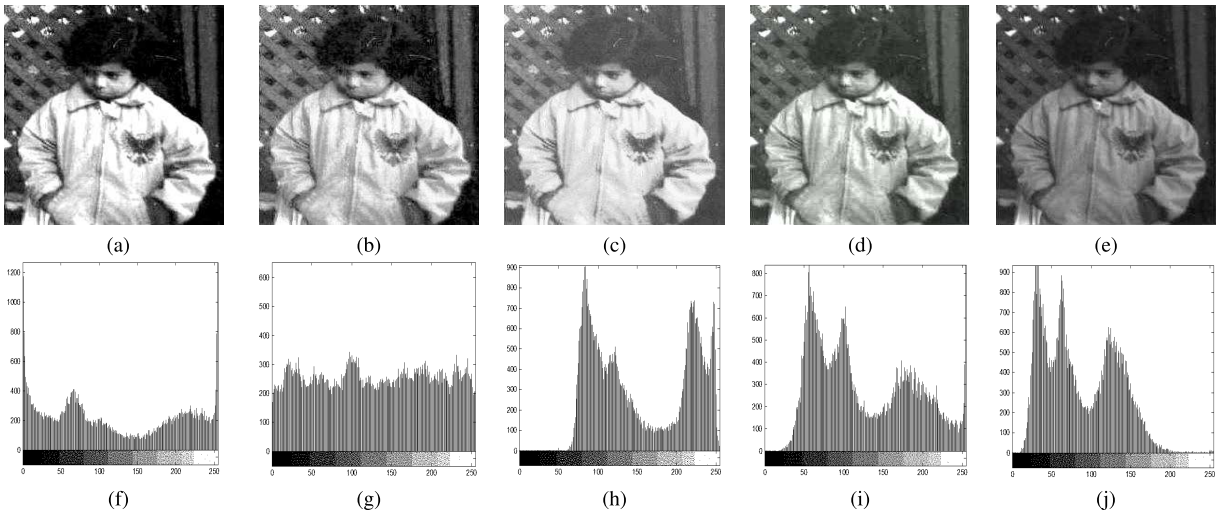


**FIGURE 5.** *CE* of Image 1 by means of (a) Prop. Proc., (b) *HE*, (c) *R*, (d) *P* and (e) *C*, and their histograms from (f) to (j), respectively.

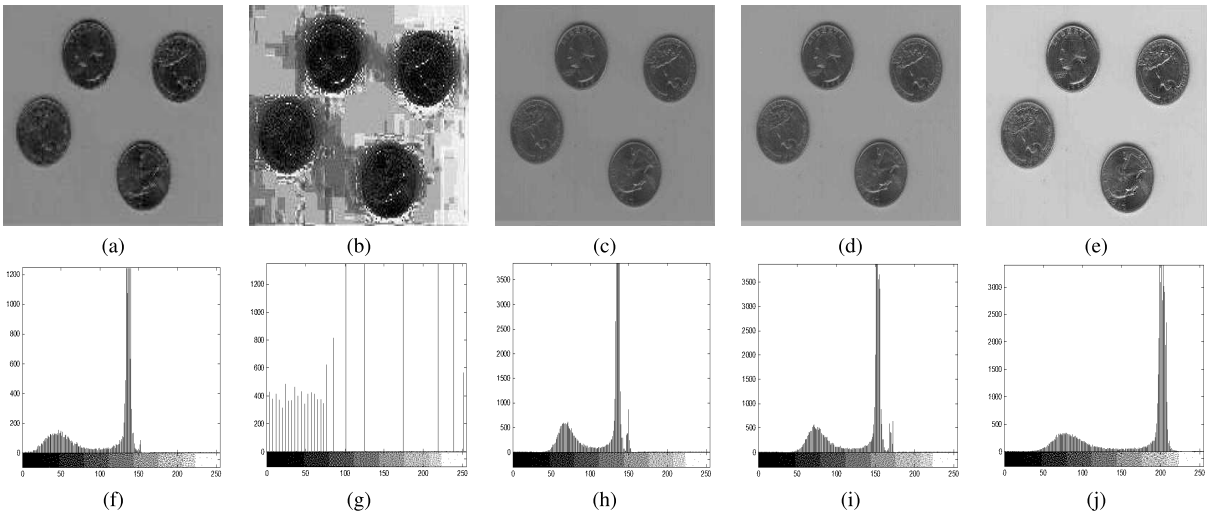


**FIGURE 6.** *CE* of Image 2 by exploiting (a) Prop. Proc., (b) *HE*, (c) *R*, (d) *P* and (e) *C*. (f) to (j) show the histrograms of (a) to (e), respectively.

**TABLE 1.** Comparison of the results obtained by the proposed procedure and by other established techniques.

| | | Prop. Proc. | $C$ [19] | $L$ [21] | $R$ [18] | $HE$ | | | Prop. Proc. | $C$ [19] | $L$ [21] | $R$ [18] | $HE$ |
|---|---|---|---|---|---|---|---|---|---|---|---|---|---|
| | EM | **5.701** | 5.698 | 5.692 | 5.681 | 5.700 | | EM | **6.059** | 6.340 | 6.356 | 5.903 | 5.984 |
| Image 1 | PSNR | **11.24** | 13.026 | 12.983 | 12.374 | 12.214 | Image 3 | PSNR | **12.853** | 13.654 | 13.056 | 12.965 | 12.785 |
| | MLI | **1.801** | 1.789 | 1.795 | 1.792 | 1.797 | | MLI | **2.056** | 2.159 | 2.126 | 2.149 | 2.149 |
| | MCI | **1.312** | 1.301 | 1.306 | 1.302 | 1.310 | | MCI | **1.698** | 1.623 | 1.642 | 1.645 | 1.621 |
| | EM | **4.112** | 6.018 | 5.991 | 5.983 | 5.975 | | EM | **5.956** | 5.873 | 5.823 | 5.793 | 5.916 |
| Image 2 | PSNR | **7.965** | 9.251 | 9.121 | 9.138 | 9.132 | Image 4 | PSNR | **11.590** | 12.486 | 12.036 | 11.843 | 11.559 |
| | MLI | **2.601** | 2.114 | 2.120 | 2.122 | 2.119 | | MLI | **1.773** | 1.745 | 1.769 | 1.765 | 1.764 |
| | MCI | **1.901** | 1.439 | 1.423 | 1.410 | 1.413 | | MCI | **1.406** | 1.398 | 1.398 | 1.389 | 1.400 |

Image 4), as shown in Fig. 4 together with their histograms, which confirm the low-contrast characteristics of each image. Figs. 5a, 6a, 7a and 8a, obtained by setting $f_1 = 0.2$ [13], shows the results of the proposed procedure in which, as indicated by the histograms, a substantial increase in contrast is detectable in all images, although we note some areas in

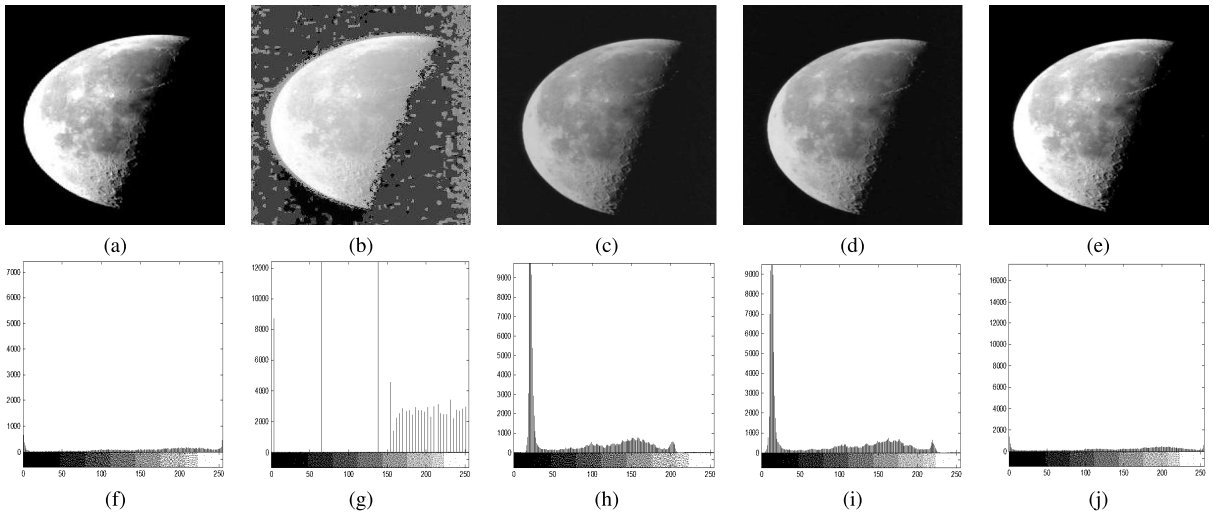


**FIGURE 7.** *CE* of Image 3 obtained by (a) Prop. Proc., (b) *HE*, (c) *R*, (d) *P* and (e) *C*, and their histograms, respectively, from (f) to (j).

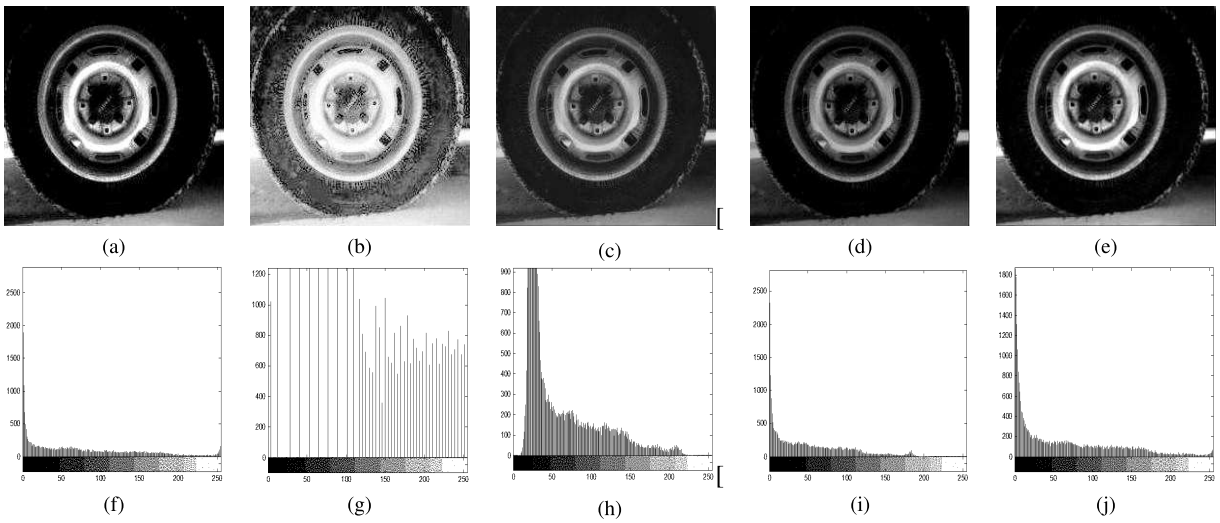


**FIGURE 8.** *CE* of Image 4 obtained by (a) Prop. Proc., (b) *HE*, (c) *R*, (d) *P* and (e) *C* for *CE* of Image 4, and their histograms from (f) to (j), respectively.

which over- and under-enhancement occur because the edited $S - SMF$ presents two cusps. However, the good quality of the obtained contrast compensates the presence of these small altered areas. After implementing the proposed procedure, the principal elements of the images are enhanced, and the contours, shadows and details are highlighted. The performance of the proposed procedure (*Prop. Proc.*) is evaluated by comparing the results with those of Cheng and Xu [19], Li *et al.* [21], Reshmalakshmi and Sasikumar [18] and histogram equalization (*HE*) approaches. Moreover, in each $4 - UKC$, the location of the individual *FP* denotes the tendency for under- and/or over-enhancement (see Fig. 2 for Image 1).[4] The obtained *CE* is also evaluated based on four metrics, namely, entropy measure (*EM*), peak signal-to-noise ratio (*PSNR*), measure of luminance index (*MLI*) and measure of contrast index (*MCI*), whose numerical results are displayed in Table 1. The high values of *EM* and *MLI* together with the small values of *PSNR* indicate a high-quality contrast. However, in confirmation of the risk of under-/over-enhancement, some of the *PSNR* values are lower than those produced by the other techniques. Similarly, the *MLI* values are slightly higher than those obtained by the alternative techniques. Figs. 5b, 6b, 7b and 8b show the results of the *HE* procedure. This procedure produced good results for images belonging to Class III, in which large dark areas and small bright areas are present (Fig. 7b). The other images (Figs. 5b, 6b and 8b), although conservative in detail, are lacking in clarity, as numerically confirmed by the results reported in Table 1. Figs. 5c, 6c, 7c and 8c

[4]The closer the *FP* is to $0_{4-UKC}$, the higher the risk of under-enhancement. Conversely, the closer *FP* is to $1_{4-UKC}$, the higher the risk of under-enhancement

present the results of Reshmalakshmi's approach [18]. Relative to the treated images, the obtained contrast lacks in quality, especially for highly detailed images (Figs. 5c and 8c), while a good contrast is produced in the remaining images. Even in these cases, the numerical results show compliance with the qualitative results (Table 1). The following set of Figures, 5d, 6d, 7d and 8d, is produced by Li's approach [21]. This approach does not produce high-quality images when there is a high level of detail in the $OI$, as indicated by both qualitative and numerical analysis. However, the procedure produced good results for images in Class III (Fig. 7d, Table 1). Finally, Figs. 5e, 6e, 7e and 8e show the results produced by Cheng's method [19].

## V. CONCLUSIONS AND PERSPECTIVES

In this paper, the problem of contrast enhancement for gray level images is solved with a new fuzzy procedure. Starting from a pixel-by-pixel scan of a normalized gray level image, a smooth S-shaped membership function is adaptively set according to both noise reduction and information loss minimization. A set of partially overlapped fuzzy patches cover the input-output space of the S-function; after appropriate fuzzification, a set of statistical features are extracted from the supports to identify the critical point characterized by the maximum fuzziness. This point give us the coexistence of fuzzy patches and the S-function and provides the point where the S-function will change its slope to implement contrast enhancement. Specifically, the fuzzified statistical features are considered as points inside a fuzzy unit hypercube, and fuzzy contrast enhancement is achieved by a weighted calculation of the distance among these points and the vertexes of the hypercube representing both the maximum brightness and maximum darkness. This procedure is implemented and applied to four classes of low-contrast images with different characteristics and the performance is evaluated with respect to four objective metrics and standard histogram comparisons. The experimental results are encouraging, as clearly demonstrated by comparison with other established fuzzy techniques and the standard histogram equalization approach. However, it should be noted that the proposed technique can produce over- and under-enhancement phenomena due to the non-differentiability of the S-function in two cusps. Therefore, future effort should be focused in this direction.

## APPENDIX
## PROOF OF THEOREM 1

Let us consider $(\underline{c}, <) = (\{c_1, c_2, c_3\}, <)$. Since $\underline{c}$ is a vector of brightness values, then

$$\begin{aligned} h_{min} < c_1 &= min(\underline{c}) < c_2 < c_3 < \ldots < c_{k-1} < c_k \\ &= max(\underline{c}) < h_{max} \end{aligned}$$

holds. If $[h_{min}, c_1]$ represents the total darkness, its membership degree is null. Therefore, $Support_1 = [h_{min}, c_1]$ gains in significance and $S(Support_1) = 0$. Clearly, $[c_{j-1}, c_j]$ with $j = 1, \ldots, k$ can be considered as supports: $Support_j = [c_{j-1}, c_j]$ with $j = 1, \ldots, k$ and $S(Support_j) \neq 0$ (particularly, $> 0$). Since $S(Support_1) = 0$ and $S(Support_j) \neq 0, \quad j = 2, \ldots, k$, we extract $k$ $n$-dimensional vectors of features, $F(Support_j)$, but $S(Support_j) > 0$ implies $F(Support_j) \neq 0$ and $F(Support_j) > 0$ is not necessary. Finally, $F(Support_1) = \underline{0}$ and $F(Support_j) \neq \underline{0}, \quad j = 2, \ldots, k$. The $k$ vectors require fuzzification, which by means of sigmoidal functions, gives us the following characterization:

$$\begin{cases} FF_{Support_1} = Sig(\underline{0}) = \underline{0} \\ FF_{Support_j} = Sig(F(Support_j)) > \underline{0}, \quad j = 2, \ldots, k. \end{cases}$$

Note that $FF_{Support_j}$ is greater than zero (for $j = 2, \ldots, k$) since fuzzification produces a mapping ranging into $n-UKC$. To obtain (3), it is sufficient to observe that, in $n - UKC$ and by a norm, for $j = 2, \ldots, k$, the relation

$$distance(FF_j, 0) = ||Sig(F(Support_j)) - Sig(\underline{0})||$$

holds and, by the considerations specified above, gives us

$$distance(FF_j, 0) \neq 0.$$

To prove that $distance(FF_j, 1_{n-UHC}) \neq 0$, it is sufficient to repeat the same path, resulting in the following implication:

$$\begin{cases} S(Support_1) = 1 \\ S(Support_j) \neq 0 \\ j = 2, \ldots, k \end{cases} \Rightarrow \begin{cases} F(Support_1) = \underline{1} \\ F(Support_j) \neq \underline{0} \\ j = 2, \ldots, k \end{cases}$$

and, after fuzzification by the $Sig$ function, it is easy to get

$$\begin{cases} FF_{Support_1} = Sig(\underline{1}) = \underline{1} \\ FF_{Support_j} = Sig(F(Support_j)) \neq \underline{0}, \quad j = 2, \ldots, k. \end{cases}$$

Finally, the purpose is obtained in terms of norms:

$$distance(FF_j, 1) = ||Sig(F(Support_j)) - Sig(\underline{1})|| \neq 0.$$

To prove that $0 < slope_{new} < \infty$, we observe that both $distance(FF_j, 1_{n-UKC})$ and $distance(FF_j, 0_{n-UKC})$ are inner ranges of $n - UKC$, so they suffer from limitations

$$\begin{cases} 0 < distance(FF_j, 1_{n-UKC}) < \sqrt{n} \\ 0 < distance(FF_j, 0_{n-UKC}) < \sqrt{n}, \end{cases}$$

(where $\sqrt{n}$ represents the diagonal length in $n - UKC$), that when divided by each other give

$$0 < \frac{distance(FFj, 1_{n-UKC})}{distance(FF_j, 0_{n-UKC})} < \infty,$$

from which the assertion follows.

## REFERENCES

[1] R. C. Gonzales and R. F. Woods, *Digital Image Processing*. New York, NY, USA: Prentice-Hall, 2007.
[2] Z. Chen, B. R. Abidi, D. L. Page, and M. A. Abidi, "Gray-level grouping (GLG): An automatic method for optimized image contrast enhancement—Part II: The variations," *IEEE Trans. Image Process.*, vol. 15, no. 8, pp. 2303–2314, Aug. 2006.
[3] W. Burger and M. J. Burge, *Principles of Digital Image Processing*. London, U.K.: Springer-Verlag, 2009.

[4] P. Soille, *Morphological Image Analysis: Principles and Applications*. Berlin, Germany: Springer, 2003.
[5] J. D. Mendiola-Santibañez, I. R. Terol-Villalobos, G. Herrera-Ruiz, and A. Fernández-Bouzas, "Morphological contrast measure and contrast enhancement: One application to the segmentation of brain MRI," *Signal Process.*, vol. 87, no. 9, pp. 2125–2150, 2007.
[6] H. Hassanpour, N. Samadiani, and S. M. M. Salehi, "Using morphological transforms to enhance the contrast of medical images," *Egyptian J. Radiol. Nucl. Med.*, vol. 46, no. 2, pp. 481–489, 2015.
[7] K. Hasikin and N. A. M. Isa, "Enhancement of the low contrast image using fuzzy set theory," in *Proc. Int. Conf. Comput. Modelling Simulation*, Cambridge, U.K., 2012, pp. 371–376.
[8] B. Madduma and S. Ramanna, "Image retrieval based on high level concept detection and semantic labelling," *Intell. Decision Technol.*, vol. 6, no. 3, pp. 187–196, 2012.
[9] B. Jayaram, K. V. V. D. L. Narayana, and V. Vetrivel, "Fuzzy inference system based contrast enhancement," in *Proc. EUSFLAT-LFA*, vol. 3. Aix-les-Bains, France, 2011, pp. 311–318.
[10] A. Taguchi, T. Kimura, and H. Tsuji, "Image enhancement of noisy images by using fuzzy data-dependent bilateral filter," in *Proc. IEEE Fuzzy Syst. Knowl. Discovery*, Tianjin, China, Aug. 2009, pp. 277–281.
[11] S. K. Pal and R. A. King, "On edge detection of X-ray images using fuzzy sets," *IEEE Trans. Pattern Anal. Mach. Intell.*, vol. PAMI-5, no. 1, pp. 69–77, Jan. 1983.
[12] S. Mukhopadhyay and B. Chanda, "A multiscale morphological approach to local contrast enhancement," *Signal Process.*, vol. 80, no. 4, pp. 685–696, 2000.
[13] J. A. Stark, "Adaptive image contrast enhancement using generalizations of histogram equalization," *IEEE Trans. Image Process.*, vol. 9, no. 5, pp. 889–896, May 2000.
[14] D. Sheet, H. Garud, A. Suveer, M. Mahadevappa, and J. Chatterjee, "Brightness preserving dynamic fuzzy histogram equalization," *IEEE Trans. Consum. Electron.*, vol. 56, no. 4, pp. 2475–2480, Nov. 2010.
[15] V. Magudeeswaran and C. G. Ravichandran, "Fuzzy logic-based histogram equalization for image contrast enhancement," *Math. Problems Eng.*, vol. 2013, Jun. 2013, Art. no. 891864.
[16] H. Lidong, Z. Wei, W. Jun, and S. Zebin, "Combination of contrast limited adaptive histogram equalisation and discrete wavelet transform for image enhancement," *IET Image Process.*, vol. 9, no. 10, pp. 908–915, 2015.
[17] H. Ibrahim and N. S. P. Kong, "Brightness preserving dynamic histogram equalization for image contrast enhancement," *IEEE Trans. Consum. Electron.*, vol. 53, no. 4, pp. 1752–1758, Nov. 2007.
[18] C. Reshmalakshmi and M. Sasikumar, "Image contrast enhancement using fuzzy technique," in *Proc. IEEE Int. Conf. Circuits, Power Comput. Technol. (ICCPCT)*, vol. 2. Mar. 2013, pp. 861–865.
[19] H. D. Cheng and H. Xu, "A novel fuzzy logic approach to contrast enhancement," *Pattern Recognit.*, vol. 33, no. 5, pp. 809–819, 2000.
[20] M. M. Gaber and H. S. Atwal, "An entropy-based approach to enhancing Random Forests," *Intell. Decision Technol.*, vol. 7, no. 4, pp. 319–327, 2013.
[21] C. Li, Y. Yang, L. Xiao, Y. Li, Y. Zhou, and J. Zhao, "A novel image enhancement method using fuzzy Sure entropy," *Neurocomputing*, vol. 215, pp. 196–211, Nov. 2016.
[22] A. S. Parihar, O. P. Verma, and C. Khanna, "Fuzzy-contextual contrast enhancement," *IEEE Trans. Image Process.*, vol. 26, no. 4, pp. 1810–1819, Apr. 2017.
[23] B. S. Khehra and A. P. S. Pharwaha, "Integration of fuzzy and wavelet approaches towards mammogram contrast enhancement," *J. Inst. Eng. (India) B*, vol. 93, no. 2, pp. 101–110, 2012.
[24] S. Patnaik and B. Zhong, Eds., *Soft Computing Techniques In Engineering Applications*. Cham, Switzerland: Springer, 2014.
[25] A. Ruano and A. R. Várkonyi-Kóczy, Eds., *New Advances in Intelligent Signal Processing* (Studies in Computational Intelligence), vol. 372. Berlin, Germany: Springer-Verlag, 2011.
[26] M. Sarkar and S. Banerjee, "Exploring social network privacy measurement using fuzzy vector commitment," *Intell. Decision Technol.*, vol. 10, no. 3, pp. 285–297, 2016.
[27] M. Versaci, S. Calcagno, and F. C. Morabito, "Fuzzy geometrical approach based on unit hyper-cubes for image contrast enhancement," in *Proc. IEEE Int. Conf. Signal Image Process. Appl. (ICSIPA)*, Kuala Lumpur, Malaysia, Oct. 2015, pp. 488–493.
[28] B. Kosko, *Fuzzy Engineering*. New York, NY, USA: Prentice-Hall, 1997.

**MARIO VERSACI** (SM'17) received the Laurea degree in civil engineering and the Ph.D. degree in electronic engineering from the Mediterranea University of Reggio Calabria, Italy, in 1994 and 1999, respectively, and the degree in mathematics from the University of Messina in 2013. He is currently serves as an Associate Professor of electrical engineering and the Scientific Head of the NDT/NDE Laboratory with the Mediterranea University of Reggio Calabria. His research focus is on soft computing techniques for NDT/NDE and image processing. He is a member of the Italian Society for Industrial and Applied Mathematics.

**FRANCESCO CARLO MORABITO** is currently a Full Professor of electrical engineering with the Mediterranea University of Reggio Calabria, Italy, and the Former Dean of the Faculty of Engineering. He is also serving as the Vice-Rector for International and Institutional Relations. He has authored or co-authored of over 350 papers in international journals/conference proceedings in various fields of engineering (radar data processing, nuclear fusion, biomedical signal processing, nondestructive testing and evaluation, and computational intelligence). He is co-author of ten books and has held three international patents. He is a Foreign Member of the Royal Academy of Doctors, Spain. He served as the Governor of the International Neural Network Society for 12 years and as the President of the Italian Network Society from 2008 to 2014. He is a member of the Editorial Boards of international journals, including the *International Journal of Information Acquisition*, *Neural Networks*, and *Renewable Energy*.

**GIOVANNI ANGIULLI** (SM'15) received the Ph.D. degree in electronic engineering and computer science from the University of Naples Federico II in 1998. Since 1999, he has been with the Mediterranea University of Reggio Calabria as an Adjunct Professor. His research interests include numerical methods and functional analysis techniques in electromagnetics. He is a member of the Institute of Electronics, Information and Communication Engineers. He currently serves as an Associate Editor for the IEEE Access.